Effect of soil water-repellent layer depth on post-wildfire hydrological processes

Article *in* Hydrological Processes · September 2019

DOI: 10.1002/hyp.13583

3 authors, including:

Jingjing Chen
Virginia Polytechnic Institute and State University
5 PUBLICATIONS **9** CITATIONS
SEE PROFILE

Ryan D. Stewart
Virginia Polytechnic Institute and State University
52 PUBLICATIONS **151** CITATIONS
SEE PROFILE

Chen Jingjing (Orcid ID: 0000-0002-5820-8360)
Stewart Ryan (Orcid ID: 0000-0002-9700-0351)

Effect of soil water-repellent layer depth on post-wildfire hydrological processes

Jingjing Chen[1*], Kevin J. McGuire[2,3], Ryan D. Stewart[1]

[1]*School of Plant and Environmental Sciences, Virginia Tech, Blacksburg, VA 24061*

[2]*Department of Forest Resources and Environmental Conservation, Virginia Tech, Blacksburg, VA 24061*

[3]*Virginia Water Resources Research Center, Virginia Tech, Blacksburg, VA 24061*

*corresponding author: jingji9@vt.edu

This article has been accepted for publication and undergone full peer review but has not been through the copyediting, typesetting, pagination and proofreading process which may lead to differences between this version and the Version of Record. Please cite this article as doi: 10.1002/hyp.13583

Abstract

Soil water repellency induced by wildfires can alter hydraulic properties and hydrologic processes; however, the persistence and vertical position (i.e., depth) of water repellent layers can vary between systems and fires, with limited understanding of how those variations affect infiltration processes. This study occurred in two forested locations in the south-central Appalachian Mountains that experienced wildfires in late 2016: Mount Pleasant Wildfire Refuge, Virginia, and Chimney Rock State Park, North Carolina. In each location, sites were selected to represent unburned conditions and low to moderate burn intensities. At each site, we measured the soil water repellency at the surface (ash layer or O horizon) and ~2 cm below the surface (A horizon) using the water drop penetration time (WDPT) method (n = 10-14). Soil water content was also measured over the upper 10 cm of the soil (n = 10), and infiltration tests were conducted using a tension infiltrometer (n = 6-8). The results showed that soil repellency was highest in the surface layer at the Mount Pleasant location and was highest in the subsurface layer at the Chimney Rock location. Soil water content was lower in unburned soil than in burned soil, especially for measurements taken immediately post-fire, with soil water content negatively correlated with water repellency. Water repellency in the surface layer significantly reduced relative infiltration rates (estimated as differences between initial and steady-state rates), whereas subsurface water repellency did not affect relative infiltration. As a result, water repellency persisted longer in sites with surface as opposed to subsurface water repellency. Finally, differences between burned and unburned sites showed that while the wildfires increased the occurrence of water repellency, they did not alter the underlying relationship between relative infiltration and water repellency of the surface soil.

Keywords: water repellency, hydrophobicity, water drop penetration time, infiltration, overland flow, soil water content, humid hardwood forests

1 Introduction

The frequency and duration of large wildfires have increased in many forest types, including humid hardwood forests, due to warmer air temperatures (Fried *et al.*, 2004; Westerling *et al.*, 2006; Dennison *et al.*, 2014; Jolly *et al.*, 2015), greater incidence and duration of drought (Siegert *et al.*, 2001), and enhanced fuel aridity (Abatzoglou and Williams, 2016). In the coming decades, global temperatures are projected to continue rising, with corresponding increases in drought conditions and wildfire occurrence (Pechony and Shindell, 2010; Schoennagel *et al.*, 2017). Wildfires can affect various hydrological processes, such as preventing soil infiltration (Ebel and Moody, 2016), increasing or reducing surface runoff (Granged *et al.*, 2011; Ebel *et al.*, 2012), and enhancing subsoil moisture storage due to reductions in transpiration (Helvey, 1980; Rye and Smettem, 2017). Wildfire can likewise modify soil hydrologic properties such as wettability (Doerr *et al.*, 2006), hydraulic conductivity (Ebel and Martin, 2017), and pore size distribution (Woods and Balfour, 2008). Fire-induced alterations in hydrological processes can negatively impact quantity and quality of water supply, thereby increasing the risk to communities that live in or near forests (Ice *et al.*, 2004; Certini, 2005; Chapin III *et al.*, 2008).

One of the most common hydrologic effects of wildfires is an increase in soil water repellency (Letey, 2001; Moody *et al.*, 2009; Granged *et al.*, 2011; Keesstra *et al.*, 2017). Wildfires often vaporize hydrophobic organic components, which can then move towards cooler spaces within the soil and condense on particle surfaces (Doerr *et al.*, 2000). Hotter soil temperatures tend to increase the depth of water repellent layers below the surface (Adams *et al.*, 1970), though the deposition process varies with confounding factors such soil water content and organic matter composition (Certini, 2005). As a result, post-wildfire soil water repellency is often irregular in terms of its location, extent and severity.

After wildfires, soils tend to have lower and more variable infiltration rates than non-burned soils, which may be caused by a water-repellent layer preventing water infiltration into deeper soil layers (DeBano, 1981; Imeson *et al.*, 1992; Ebel *et al.*, 2012). This effect is most often noted when water repellency occurs at the soil surface as opposed to the subsurface (Mansell, 1970; Prima *et al.*, 2017; Yi *et al.*, 2017), suggesting that the depth of water-repellent layers may be an important factor in post-fire hydrological processes. Still, we currently possess insufficient understanding of how the depth and persistence of water repellent soil layers affect soil water content and infiltration partitioning.

When water repellency occurs at the soil surface, infiltration measurements can help to assess the strength and persistence of the repellency (Lichner *et al.*, 2013; Alagna *et al.*, 2018). As an example, the ratio of soil-ethanol to soil-water sorptivities determined through two infiltration tests can be converted into an index of soil water repellency (Tillman *et al.*, 1989). Similarly, Alagna *et al.* (2018) developed a water repellency index estimated by a tension infiltration. The index was shown to correlate well with water repellency measures such as the water drop penetration time and ethanol to water sorptivity ratios, but the method requires linearizing the infiltration data (a process filled with ambiguity, particularly when water repellency is dynamically changing) and includes several unknown or uncertain parameters.

The effects of soil water repellency on infiltration can also be assessed using archetypal infiltration curves (**Figure 1**). Imeson *et al.* (1992) identified four curves: Type 1) *exponential decrease*, also known as the standard curve, where the infiltration rate decreases exponentially as a function of time; Type 2) *linear decrease*, where the infiltration rate linearly decreases over some period of time; Type 3) *initial increase to decrease*, where the infiltration rate first increases as a function of time before subsequently decreasing; and Type 4) *initial increase to steady state*, which is similar to Type 3, but the infiltration rate eventually reaches a steady

state that is typically greater than the initial infiltration rate. Pierson *et al.* (2008) and Pierson *et al.* (2001) presented another pattern: Type 5) *exponential decrease to linear increase*, where the infiltration rate exponentially decreases to a minimum and then linearly increases for a period of time. Types 1 and 2 are associated with hydrophilic soils and Types 3-5 indicate soil water repellency. Further, Types 1 and 4 include both transient (i.e., short-time) and steady-state (i.e., long-time) infiltration, whereas the other three types only include transient data. Pierson *et al.* (2008) also developed an infiltrability index (called INI) that is calculated as the difference of the final and minimum infiltration rates divided by final infiltration rate. This particular index was designed for Type 4 (i.e., *initial increase to steady state*) and Type 5 (i.e., *exponential decrease to linear increase*) curves, but may not differentiate between the other three curve types. Specifically, any infiltration test in which the lowest infiltration rate occurs at the end (i.e., the final infiltration rate is the minimum rate) will have an INI value of 0, regardless of the initial infiltration patterns. The INI index also does not distinguish between transient and steady-state data, meaning that the calculated value may vary depending on the duration of each infiltration test.

In this present study, we aimed to better quantify and describe water repellency effects on water infiltration, focusing on forested soils in the south-central Appalachian Mountains that were affected by wildfires in late 2016. We had two specific objectives: 1) compare the depth and severity of water repellent layers in burned soils that had experienced different fire severities versus unburned soils; and 2) quantify the effect of surface versus subsurface water repellency on near-saturated infiltration processes. As part of this analysis, we also a proposed new diagnostic index for identifying surface water repellency based on the relative rates of early-time and steady state infiltration, and another metric based on the time to maximum infiltration rate. Altogether, this study seeks to generate new understanding regarding the role of water repellent soil layers on hydrological response to wildfire.

2 Methods

2.1 Sampling Sites

We selected two locations in the Blue Ridge physiographic province of the south-central Appalachian Mountains (**Figure 2**): Mount Pleasant Wildlife Refuge, Virginia (37.73, -79.21), and Chimney Rock State Park, North Carolina (35.47, -82.24). Elevations are approximately 730 m in Mount Pleasant and 1040 m in Chimney Rock. The climate in these two locations is temperate, with distinct summer and winter seasons. The vegetation at Mount Pleasant is mostly hardwood, comprised of chestnut oak (*Quercus prinus*), red oak (*Quercus rubra*), and white oak (*Quercus alba*), with some white pine (*Pinus strobus*) and sugar maple (*Acer saccharum*). The Chimney Rock location is characterized by Montane Oak-Hickory (*Quercus alba* - *Quercus* (*rubra, montana*) / *Rhododendron calendulaceum* - (*Gaylussacia ursina*); NCDENR, 2011) and Pine-Oak/Heath forests (*Pinus pungens* - *Pinus rigida* - (*Quercus montana*) / *Kalmia latifolia* - *Vaccinium pallidum*). Mountain laurel (*Kalmia latifolia*) is the primary understory species at both locations. The dominant bedrock at the Mount Pleasant is granitic and the soils are fine-loamy Ultisols. The dominant bedrock at Chimney Rock is gneiss and the soils are coarse-loamy Inceptisols (NRCS, 2017).

Fires occurred from 21 November to 25 November 2016 in Mount Pleasant, during which time 4,536 hectares were burned. In Chimney Rock, fires burned 3,210 hectares between 8 November and 28 November 2016 (Tobin *et al.*, 2016). In each location, we selected sites to represent unburned conditions along with two different burn severities (MTBS, 2018). In Mount Pleasant, we randomly selected four sites on the midslopes and shoulders of west-facing slopes that spanned a gradient of fire severity: M1 represented low fire severity, M2 represented low to moderate severity, and M3 and M4 were unburned sites. M3 was located on the upper side of M1, and M4 was located adjacent to M2. M3 and M4 were smaller in area than M1 and

M2. In Chimney Rock, we randomly selected three sites: C1 represented low fire severity, C2 represented moderate severity, and C3 acted as unburned control. C1 was located on an east-facing mid-slope, C2 was located on an east-facing shoulder slope, and C3 was located on the mountain ridge; the three sampling sites here had approximately equal areas. Fire intensity was estimated using MODIS Fire Radiation Power (FRP) data (Giglio *et al.*, 2016).

Soil properties, plants species, and wildfire characteristics in each location are summarized in **Table 1**.

2.2 Measurements

Measurements were collected between November 2016 and January 2018. In Mount Pleasant, measurements were conducted every one to two months (8 times total); in Chimney Rock, measurements were collected every three months (4 times total). On each sampling date, 10 measurement points were tested per site. Sample points in M1, M2, C1, C2, and C3 were located in an approximately rectangular grid with sampling points spaced 2-3 m apart. Sample points in M3 and M4 were also selected in an approximately rectangular grid; however, due to the relatively small sampling areas in those sites, points were spaced 1-2 m from each other. Points were randomly selected on each sampling date.

At each sample point, soil water repellency was quantified using the water drop penetration time (WDPT) test (Dekker *et al.*, 2009) and mini-disk infiltrometer (Robichaud *et al.*, 2008). Prior to the drop and infiltration tests, the soil surface was cleaned of any loose leaf and duff materials, thus exposing either the upper ash layer (burned sites) or organic horizon (unburned sites). Drop tests were first conducted on this top layer, then conducted on the layer where the soil was excavated down to a depth of ~2 cm, which represented the transition between ash and mineral layers (burned sites) and A to O horizons (unburned sites). At each measurement point,

5-7 WDPT tests were performed at the surface and another 5-7 WDPT tests were performed in the shallow subsurface (~2 cm depth). Test results were classified into one of two categories: WDPT < 10 s and WDPT ≥ 10 s (Adams *et al.*, 1970). Water repellency, *WR*, was then quantified on a given sampling date as the percentage of WDPT tests ≥ 10 s for each measurement point, with WR_s representing water repellency at the land surface and WR_{sub} representing water repellency at the ash-mineral soil interface in burned sites and at a similar depth in unburned sites. Note that each measurement point could have discrete *WR* values from 0% to 100%, depending on how many of the 5-7 drops at each depth persisted for longer than 10 s.

Infiltration tests (n = 6-8) were conducted on the surface layer using a mini-disk tension infiltrometer with a disk diameter of 4.5 cm (METER Group, Inc. Pullman, WA, USA). The infiltrometer was set to -1 cm tension during runs. A thin layer of coarse sand (20/30 mesh) was applied as needed to level the measured surface. Infiltrated water volumes were recorded every 0.5 minutes, with measurements continuing until the rates were within ± 5% of one another for three consecutive readings. All of the infiltration tests were conducted immediately adjacent to the drop tests. In addition, soil water content for each sample point was measured using a GS3 probe and ProCheck reader (METER Group, Inc. Pullman, WA, USA).

Unconsolidated soil samples and intact soil cores were also collected on each sampling date. The unconsolidated samples were analyzed for total organic carbon using a C/N analyzer (VarioMax CNS macro-element analyzer, Elementary Analytical Systems GmbH, Hanau, Germany), soil pH using a 3100M meter (OHAUS, Inc., Parsippany, USA), and particle size distribution following the procedures recommended by Klute and Dinauer (1986) and using a CILAS 1190 Particle Size Analyzer (CILAS, Inc., Orleans, France). Soil bulk density was determined from the cores after oven-drying for 24 hours at 105 °C (Blake, 1965).

2.3 Analysis

Relative infiltration rate (*RI*) was quantified using the tension infiltrometer readings as

$$RI = \frac{i_i - i_{ss}}{i_i + i_{ss}} \quad (1)$$

where i_i is the initial infiltration rate (taken here from the first three readings, which occurred over a 1.5 min period) and i_{ss} is the final infiltration rate (taken here as the last three readings when the infiltration rate reaches steady-state, also over a 1.5 min period; **Figure 1f**). *RI* can range from -1 to 1, with a value of $RI = 0$ indicating that the initial and final infiltration rates were equal, $-1 \leq RI < 0$ indicating that the initial infiltration rate was less than final infiltration rate, and $0 < RI \leq 1$ indicating that the initial infiltration rate was greater than final infiltration rate. The time at which the maximum infiltration rate occurred was also recorded.

The measured soil water repellency (*WR*) and relative infiltration rate (*RI*) data did not conform to the assumptions of normality and homogeneity; thus, nonparametric approaches were used for comparison. For *WR*, the median value from the 10 measurement points per site and sampling data was recorded, while the median value from 3-6 measurements per site and sampling date is shown for *RI*. The 95% confidence intervals were estimated for each median value using the Wilcoxon procedure. A non-parametric Kruskal-Wallis test with Mann-Whitney U (K-W with MU) post hoc analysis was used to compare *WR* and *RI* values between sites. *WR* differences between soil positions (surface = WR_s; subsurface = WR_{sub}) were analyzed by using the Mann-Whitney U test (MU) if the K-W test was significant. Water content data were normal and homogeneous; thus, sites were compared for each location using a one-way Analysis of Variance (ANOVA) with Tukey honestly significant difference (HSD) post hoc analysis. Linear relationships between the relative infiltration rates (*RI*), water contents, and relative soil water repellency at each depth (WR_s and WR_{sub}) were examined using Pearson's

correlation and Analysis of Covariance (ANCOVA), because the residual errors were normal and homogeneous. Differences and correlations were considered significant for $p \leq 0.05$. R (version 3.5.1) was used for all statistical analyses.

3 Results

3.1 Soil water repellency

In both locations, soils that experienced low and moderate burn severities showed evidence of water repellency (**Figure 3**). Burned soils in the M2 (low-moderate severity) and C2 (moderate severity) sites were generally more water repellent than in the M1 and C1 sites (both low severity burns). Unburned soils were hydrophilic (*WR* = 0%), with the exception of the August and October 2017 measurements in Mount Pleasant, when the unburned soils showed *WR* values from 60-100%.

The depth distributions of water repellency differed between the two locations. In Mount Pleasant, the relative water repellency on the soil surface was significantly greater than in the subsurface layer (mean WR_s = 55.4% $\pm$ 2.5% standard error; mean WR_{sub} = 32.5% $\pm$ 2.7% standard error; MU, $p < 0.05$). The M2 site showed significantly higher relative surface water repellency (WR_s) than the M1 site (K-W with MU, $p < 0.05$). In the subsurface soil layer, WR_{sub} was generally less than in the surface soil layer, and only showed a significant difference between fire severities in March 2017. In Chimney Rock, surface soils were rarely water repellent (mean WR_s = 7.47%), while the burned subsurface soils showed water repellency (mean WR_{sub} = 41.6%). WR_{sub} was significantly different between fire severities in the first two measurements (January and June 2017), as the moderate burned (C2) soil had significantly greater WR_{sub} than the low severity burned (C1) soil (K-W with MU, $p<0.05$). The unburned soil in Chimney Rock was hydrophilic for all measurements (*WR* = 0.0%).

3.2 Soil water content

Water contents in the low-moderate/moderate burned soils (M2, C2) at both locations were significantly lower than in the unburned soils for the majority of measurements (ANOVA with Tukey HSD, $p < 0.05$; **Figure 4**). In Mount Pleasant, soil water contents ranged from 0.06 to 0.39 cm^3 cm^{-3} (**Figure 4a**). The M2 site had lowest water contents, with the exception of the late summer/early fall of 2017 (August 2017 and October 2017), when all soils were dry. The unburned soils (M3 and M4) had the highest water contents. In Chimney Rock, soil water contents ranged from 0.05 to 0.35 cm^3 cm^{-3} (**Figure 4b**). Here, with the exception of the last measurement (January 2018), the moderately burned site (C2) had significantly lower water contents than the C1 and C3 sites. At both locations, soil water contents in the low-severity burned soils (M1 and C1) had the largest variation, yet these soils generally had water content values that were between those of the unburned soils (M3, M4, and C3) and low-moderate/moderate burned soils (M2 and C3).

3.3 Infiltration tests

Tension infiltration measurements, conducted using a source tension of -1 cm, revealed different patterns of soil water infiltration rates as functions of time in burned and unburned sites (**Figure 1g**). In the unburned sites, most infiltration tests showed the standard behavior (i.e., Type 1 curve), in which infiltration rate exponentially decreased with time before reaching steady-state (**Figure 1a**). In the burned sites, by contrast, infiltration rates were typically low at the beginning of the test before increasing to maximum values and then declining to steady-state rates, thus resembling the Type 4 curve (**Figure 1d**).

Relative soil water infiltration rate (*RI*) changed through time after wildfires and was affected by fire severity (**Figure 5**). The infiltration tests conducted in February 2017 at Mount Pleasant

showed that *RI* was < 0 for the burned sites (M1 and M2), meaning that final, steady-state infiltration rates exceeded initial rates. The unburned sites (M3 and M4) had *RI* values > 0 on that same date. While the low-severity burn site (M1) shifted to *RI* > 0 in subsequent months, the low-moderate burn severity site M2 maintained median *RI* values ≤ 0 for all but the final measurement (conducted in December 2017). Site M2 had significantly lower *RI* values than the other sites in March, May and June 2017, though no significant differences were observed between sites in the measurements taken in August, October and December 2017. Chimney Rock had median *RI* values that were all > 0, indicating that the initial infiltration rates were greater than the final infiltration rates. No significant differences in *RI* were detected between sites.

3.4 Correlations between variables

In all burned sites, soil water repellencies in the surface and subsurface layers were negatively correlated with soil water content (Pearson r_p = -0.85 to -0.79 in Mount Pleasant and r_p = -0.77 to -0.74 in Chimney Rock; **Figure 6**). Soil water content and soil water repellency had significant individual linear relationships for all sites except the unburned site at Chimney Rock (ANCOVA; $p < 0.05$). However, the slopes between these linear models did not significantly differ between sites (p_{slope} = 0.22 and $p_{intercept}$ = 0.42 in Mount Pleasant; p_{slope} = 0.17 and $p_{intercept}$ = 0.07 in Chimney Rock). This result suggests that the fires did not significantly alter this relationship at Mount Pleasant, and that fire severity was not a significant factor in Chimney Rock.

The time for infiltration tests to reach their maximum rates was affected by surface water repellency, with higher WR_s values associated with longer times to maximum infiltration rate (**Figure 7a**). By contrast, the time to maximum infiltration rates did not show any relationship with WR_{sub} (**Figure 7b**). *RI* also had a significant and negative correlation to WR_s (Pearson; r_p

= - 0.61, $p < 0.05$; **Figure 8a**). This relationship was most evident in the Mount Pleasant location, where low-moderate severity burn site (M2) had the highest WR_s values along with the lowest *RI* values. The unburned sites (M3 and M4) also showed relatively high WR_s and relatively low *RI* values in August and October 2017, due to dry soil conditions. The ANCOVA analysis indicated that *RI* was linearly correlated with WR_s in both burned and unburned sites ($p < 0.05$); however, the slopes ($p = 0.20$) and intercepts ($p = 0.14$) of linear models in burned and unburned sites were not significantly different. *RI* showed no significant relationship to WR_{sub} (**Figure 8b**).

4 Discussion

The two locations studied here showed considerable differences in the depth and persistence of water repellency after the fires. In Mount Pleasant, the surface ash layer showed significantly higher water repellency than the ash-mineral soil interface layer (**Figure 3a**). During the summer and early fall of 2017, the unburned soils also became dry and water repellent, due to natural repellency that, for example, can be induced by active fungi in these warmer period (Feeney *et al.*, 2006). This finding of soil water repellency in unburned soils is consistent with observations from coniferous (Woods *et al.*, 2007; Granged *et al.*, 2011) and Eucalyptus forests (Doerr *et al.*, 2006) and shrublands (Keesstra *et al.*, 2017). However, such observations are rare in humid hardwood forests, and in this instance may be due to organic substances that had leached out of the O horizon to the surface of the A horizon, where our measurements were collected. At the same time, the water repellency data collected here revealed that even though the burned soils tended to be drier (**Figure 4**) and possess more consistent water repellency (**Figure 3**), the wildfire did not fundamentally change the relationship between relative water repellency and water content (**Figure 6a**).

In the two burned sites at Chimney Rock (C1 and C2), the subsurface ash-soil interface layer had greater water repellency than the surface ash layer (**Figure 3d**). Here the soil water repellency decreased through time, such that by one year after the fire water repellency was only observed in a few places within the moderate burn severity (C2) site. The unburned site (C3) never exhibited water repellency. As a consequence, the wildfires in this forest appear to have altered the relationship between water content and relative water repellency (**Figure 6b**), even though burn severity was determined to not be a significant factor in that response.

The differences in the depth of water repellency layers between Mount Pleasant and Chimney Rock may relate to variations in fire temperatures and duration, as well as soil texture differences. In Chimney Rock, the fire had higher radiative power and resulted in greater burn intensity compared to Mount Pleasant (**Table 1**), making it possible that the more organic matter was volatilized during fire (Simkovic *et al.*, 2008; Stoof *et al.*, 2010). Also, the coarser textured sandy loam soil Chimney Rock likely had greater thermal diffusivity and conductivity, and less volumetric heat capacity, than the finer textured loam soil in Mount Pleasant (Al Nakshabandi and Kohnke, 1965; Abu-Hamdeh, 2003; Nikoosokhan *et al.*, 2015), meaning that the heat from the fire could have reached to deeper depths in the soil. Since vaporized hydrophobic compounds condense in cool areas of the soil (DeBano *et al.*, 1970; Certini, 2005), this process could explain the formation of subsurface water repellency seen in Chimney Rock and surface water repellency in Mount Pleasant.

Wildfires can reduce water infiltration rates, as has been demonstrated in previous studies (Imeson *et al.*, 1992; Larsen *et al.*, 2009; Moody *et al.*, 2009; Granged *et al.*, 2011). The Mount Pleasant location showed a similar response, in which the burned sites had relative infiltration (*RI*) values < 0 after fire (**Figure 5a**). Still, the unburned soils at that location also showed *RI* < 0 during times when the surface layer became water repellency (i.e. $WR_s > 0$). As a result,

the significant relationship between WR_s and *RI* did not differ between burned and unburned soils (**Figure 8a**). The infiltration tests conducted at Chimney Rock showed no differences in *RI* between burned and unburned sites (**Figure 5b**), even though there was a detectable water-repellent layer located in the sublayer soil (**Figure 3d**). Taken together, these results indicate that water repellency at the soil surface reduced initial infiltration rates (**Figure 8a**) and delayed the time to maximum infiltration rates (**Figure 7a**), whereas subsurface water repellency did not affect the initial infiltration process (**Figures 7b and 8b**).

These results suggest that, as long as a hydrophilic surface layer provides sufficient pore space, water can infiltrate into the soil without initial restriction. If a continuous hydrophilic layer exists at the surface, water may be able to move down-gradient, thus creating the possibility of lateral subsurface flow occurring above the hydrophobic layer (Yi *et al.*, 2017). In addition, fine-size ash particles can increase water retention in the surface layers (Stoof *et al.*, 2010) and can delay and reduce runoff generation (Neary *et al.*, 1999; Stoof *et al.*, 2010; Woods and Balfour, 2010). Here we speculate that higher water retention within a hydrophilic surface layer may increase wetness at the interface with a hydrophobic subsurface layer, which could lead to more rapid decreases in water repellency. Leaching of organic hydrophobic substances from water percolation has been considered to be an important factor contributing to the breakdown of soil water repellency (Doerr and Thomas, 2000); therefore, infiltration into a hydrophilic surface layer may enhance these leaching and breakdown processes. Together, the high surface infiltrability in the Chimney Rock soils may have reduced the persistence of fire-induced soil water repellency in that location compared to Mount Pleasant.

The infiltration experiments were conducted using a tension infiltrometer; because the water supply is under a negative pressure in such tests, soil capillarity (i.e., sorptivity) typically provides a large contribution to total flow. Previous research has suggested that water

repellency decreases soil sorptivity by increasing the contact angle between water and solid particles (Tillman *et al.*, 1989), which could explain why the initial infiltration rates were relatively low in soils with high surface water repellency (**Figure 2**). The relationships found here between WR_s and both time to maximum infiltration rate (**Figure 7**) and *RI* (**Figure 8**) also suggest that tension infiltration tests may be useful to identify dynamics in water repellency, even when not used in conjunction with ethanol measurements (Tillman *et al.*, 1989).

Here we note that our proposed *RI* metric was designed to work with Type 1 and Type 4 infiltration curves, due to the assumption that infiltration rates have reached steady-state by the end of the measurement. This condition differentiates *RI* from other indices (e.g., the INI metric; Pierson *et al.*, 2008), and in theory should provide consistent results as the final infiltration rate will not depend on the sampling duration, unlike infiltration tests that only include the transient infiltration phase. In theory, steady-state conditions can take hours to develop and may require homogeneous conditions in the soil profile (Stewart and Abou Najm, 2018), yet in practice the infiltration measurements collected in this study all met the stated threshold for steady-state (i.e., three consecutive measurements within ± 5% of one another) within the first 90 minutes. This criterion therefore appears to be appropriate for estimating *RI*, and does not place an excess burden in terms of measurement time requirements.

We also note that the tension infiltrometer used in this study measured infiltration rates at a small scale (i.e., point scale), as the disk had a diameter of 4.5 cm. We collected 6-8 measurements per site per sampling time in an attempt to account for possible spatial variability, yet it is still unclear whether these small-scale measurements provided an accurate representation of the larger (e.g., hillslope) scale response to the fires. Previous work has shown notable scale-dependence of soil properties like saturated hydraulic conductivity (Nyman *et*

al., 2010; Ebel and Martin, 2017), so it is possible that soil water repellency exhibits similar scale-dependent effects on water movement. Also, it should be noted that the sampling densities varied in the Mount Pleasant location: sample points in the burned sites (M1 and M2) had greater spacing than in the control sites (M3 and M4), which may also influence the ability to upscale the observations collected in this study.

Over the coming decades, wildfire activity is predicted to increase in the southern Appalachian Mountains (Kang and Sridhar, 2017). While fires occurred frequently in this region until the late 1800s, subsequent suppression activities reduced wildfire incidence and extent (Lafon *et al.*, 2017). The resulting rarity of intense fires across the entire eastern United States has limited the opportunity to study if and how water repellency and infiltration processes are altered by wildfires (Kolka, 2012). The results of this study therefore provide important insight into post-fire hydrologic effects within humid hardwood forests, and suggest that even low-to-moderate wildfire severities may alter rainfall-runoff relationships in this region.

5 Summary and Conclusion

In this study, we quantified soil water repellency, water content, and relative infiltration in two south-central Appalachian Mountains locations that experienced wildfires in late 2016. Our study had two objectives: 1) compare the depth and severity of water repellent layers in burned soils that had experienced different fire severities and unburned soils; and 2) quantify the effect of surface versus subsurface water repellency on near-saturated infiltration processes.

We met Objective 1 by repeatedly measuring water drop penetration times (WDPT) at multiple sites at both locations. Based on those measurements, we found that wildfires induced soil water repellency in these humid hardwood forests. However, the depth of water repellent layers differed between the two locations, with the lower burn intensity location (Mount Pleasant,

VA; FRP = 16.2 MW) showing repellency primarily at the soil surface and the higher burn intensity location (Chimney Rock, NC; FRPs = 90.6 MW) showing repellency primarily in the subsurface (2-5 cm depth). In both locations, soil water repellency was negatively correlated with water content.

We met Objective 2 by comparing relative water infiltration rates using a tension infiltrometer. Using a new infiltration index that compared initial and steady-state infiltration rates, we found that water infiltration was initially inhibited when the soil surface was water repellent. Soils with water repellency confined to the subsurface did not show the same reductions in initial infiltration, suggesting that a thin hydrophobic soil layer at the surface may provide opportunity for water to infiltrate. This infiltrated water may then enhance the breakdown of water repellency in the subsurface.

The differences in depths of water-repellent layer may also explain why the more severely burned location (Chimney Rock) experienced limited and short-lived differences in soil water contents and relative infiltration rates after the fires, while the less severely burned (Mount Pleasant) location still showed significant differences between burned and unburned sites more than one year post-fire. Given these results, we propose that depth of a water-repellent layer is an important factor to include when assessing hydrological effects of wildfires.

Acknowledgement

Support for this project came from the Virginia Tech Institute for Critical Technology and Applied Science (VT-ICTAS). Funding for this work was provided in part by the Virginia Agricultural Experiment Station and the Hatch Program of the National Institute of Food and Agriculture, U.S. Department of Agriculture.

Data Availability Statement

The data that support the findings of this study are available from the corresponding author upon reasonable request.

References

Abatzoglou JT, Williams AP. 2016. Impact of anthropogenic climate change on wildfire across western US forests. Proceedings of the National Academy of Sciences, 113: 11770-11775.

Abu-Hamdeh NH. 2003. Thermal properties of soils as affected by density and water content. Biosystems engineering, 86: 97-102.

Adams S, Strain B, Adams M. 1970. Water‐repellent soils, fire, and annual plant cover in a desert scrub community of southeastern California. Ecology, 51: 696-700.

Al Nakshabandi G, Kohnke H. 1965. Thermal conductivity and diffusivity of soils as related to moisture tension and other physical properties. Agricultural Meteorology, 2: 271-279.

Alagna V, Iovino M, Bagarello V, Mataix-Solera J, Lichner Ľ. 2018. Alternative analysis of transient infiltration experiment to estimate soil water repellency. Hydrological Processes: 167. DOI: 10.1002/hyp.13352.

Blake G. 1965. Bulk Density 1. Methods of soil analysis. Part 1. Physical and mineralogical properties, including statistics of measurement and sampling: 374-390.

Certini G. 2005. Effects of fire on properties of forest soils: a review. Oecologia, 143: 1-10.

Chapin III FS, Trainor SF, Huntington O, Lovecraft AL, Zavaleta E, Natcher DC, McGuire AD, Nelson JL, Ray L, Calef M. 2008. Increasing wildfire in Alaska's boreal forest: pathways to potential solutions of a wicked problem. BioScience, 58: 531-540.

DeBano L, Mann L, Hamilton D. 1970. Translocation of Hydrophobic Substances into Soil by Burning Organic Litter 1. Soil Science Society of America Journal, 34: 130-133.

DeBano LF. 1981. Water repellent soils: a state-of-the-art. Gen. Tech. Rep. PSW-46. Berkeley, Calif.: US Department of Agriculture, Forest Service, Pacific Southwest Forest and Range Exp. Stn. 21 p, 46.

Dekker LW, Ritsema CJ, Oostindie K, Moore D, Wesseling JG. 2009. Methods for determining soil water repellency on field‐moist samples. Water resources research, 45.

Dennison PE, Brewer SC, Arnold JD, Moritz MA. 2014. Large wildfire trends in the western United States, 1984–2011. Geophysical Research Letters, 41: 2928-2933.

Doerr S, Shakesby R, Blake W, Chafer C, Humphreys G, Wallbrink P. 2006. Effects of differing wildfire severities on soil wettability and implications for hydrological response. Journal of Hydrology, 319: 295-311.

Doerr SH, Shakesby R, Walsh R. 2000. Soil water repellency: its causes, characteristics and hydro-geomorphological significance. Earth-Science Reviews, 51: 33-65.

Doerr SH, Thomas AD. 2000. The role of soil moisture in controlling water repellency: new evidence from forest soils in Portugal. Journal of Hydrology, 231: 134-147.

Ebel BA, Martin DA. 2017. Meta‐analysis of field‐saturated hydraulic conductivity recovery following wildland fire: Applications for hydrologic model parameterization and resilience assessment. Hydrological Processes.

Ebel BA, Moody JA. 2016. Synthesis of soil‐hydraulic properties and infiltration timescales in wildfire‐affected soils. Hydrological Processes, 31: 324-340.

Ebel BA, Moody JA, Martin DA. 2012. Hydrologic conditions controlling runoff generation immediately after wildfire. Water Resources Research, 48.

Feeney DS, Hallett PD, Rodger S, Bengough AG, White NA, Young IM. 2006. Impact of fungal and bacterial biocides on microbial induced water repellency in arable soil. Geoderma, 135: 72-80.

Fried JS, Torn MS, Mills E. 2004. The impact of climate change on wildfire severity: a regional forecast for northern California. Climatic change, 64: 169-191.

Giglio L, Schroeder W, Justice CO. 2016. The collection 6 MODIS active fire detection algorithm and fire products. Remote Sensing of Environment, 178: 31-41.

Granged AJ, Jordán A, Zavala LM, Bárcenas G. 2011. Fire‐induced changes in soil water repellency increased fingered flow and runoff rates following the 2004 Huelva wildfire. Hydrological Processes, 25: 1614-1629.

Helvey J. 1980. Effects of a North Central Washington Wildfire on Runoff and Sediment Production 1. Journal of the American Water Resources Association, 16: 627-634.

Ice GG, Neary DG, Adams PW. 2004. Effects of wildfire on soils and watershed processes. Journal of Forestry, 102: 16-20.

Imeson A, Verstraten J, Van Mulligen E, Sevink J. 1992. The effects of fire and water repellency on infiltration and runoff under Mediterranean type forest. Catena, 19: 345-361.

Jolly WM, Cochrane MA, Freeborn PH, Holden ZA, Brown TJ, Williamson GJ, Bowman DM. 2015. Climate-induced variations in global wildfire danger from 1979 to 2013. Nature communications, 6: 7537.

Kang H, Sridhar V. 2017. Combined statistical and spatially distributed hydrological model for evaluating future drought indices in Virginia. Journal of Hydrology: Regional Studies, 12: 253-272.

Keesstra S, Wittenberg L, Maroulis J, Sambalino F, Malkinson D, Cerdà A, Pereira P. 2017. The influence of fire history, plant species and post-fire management on soil water repellency in a Mediterranean catchment: The Mount Carmel range, Israel. Catena, 149: 857-866.

Klute A, Dinauer RC. 1986. Physical and mineralogical methods. Planning, 8: 79.

Kolka R. 2012. Effects of fire and fuels management on water quality in eastern North America. In: LaFayette, Russell; Brooks, Maureen T.; Potyondy, John P.; Audin, Lisa; Krieger, Suzanne L.; Trettin, Carl C. Eds. 2012. Cumulative watershed effects of fuel management in the Eastern United States. Gen. Tech. Rep. SRS-161. Asheville, NC: US Department of Agriculture Forest Service, Southern Research Station. 282-293., 161: 282-293.

Lafon CW, Naito AT, Grissino-Mayer HD, Horn SP, Waldrop TA. 2017. Fire history of the Appalachian region: a review and synthesis.

Larsen IJ, MacDonald LH, Brown E, Rough D, Welsh MJ, Pietraszek JH, Libohova Z, Benavides-Solorio JD, Schaffrath K. 2009. Causes of Post-Fire Runoff and Erosion: Water Repellency, Cover, or Soil Sealing? Soil Science Society of America Journal, 73: 1393-1407. DOI: 10.2136/sssaj2007.0432.

Letey J. 2001. Causes and consequences of fire‐induced soil water repellency. Hydrological Processes, 15: 2867-2875. DOI: 10.1002/hyp.378.

Lichner L, Hallett PD, Drongová Z, Czachor H, Kovacik L, Mataix-Solera J, Homolák M. 2013. Algae influence the hydrophysical parameters of a sandy soil. Catena, 108: 58-68.

Mansell R. 1970. Infiltration of water into soil columns which have a water-repellent layer. In: Soil Crop Sci Soc Fla Proc.

Moody JA, Kinner DA, Úbeda X. 2009. Linking hydraulic properties of fire-affected soils to infiltration and water repellency. Journal of Hydrology, 379: 291-303.

MTBS. 2018. Monitoring Trends in Burn Severity. USGS, USDA (eds.).

Neary DG, Klopatek CC, DeBano LF, Ffolliott PF. 1999. Fire effects on belowground sustainability: a review and synthesis. Forest ecology and management, 122: 51-71.

Nikoosokhan S, Nowamooz H, Chazallon C. 2015. Effect of dry density, soil texture and time-spatial variable water content on the soil thermal conductivity. Geomechanics & Geoengineering, 11: 149-158.

NRCS. 2017. Web Soil Survey. USDA (ed.).

Nyman P, Sheridan G, Lane PN. 2010. Synergistic effects of water repellency and macropore flow on the hydraulic conductivity of a burned forest soil, south‐east Australia. Hydrological Processes, 24: 2871-2887.

Pechony O, Shindell DT. 2010. Driving forces of global wildfires over the past millennium and the forthcoming century. Proceedings of the National Academy of Sciences, 107: 19167-19170.

Pierson F, Robichaud P, Moffet C, Spaeth K, Williams C, Hardegree S, Clark P. 2008. Soil water repellency and infiltration in coarse-textured soils of burned and unburned sagebrush ecosystems. Catena, 74: 98-108.

Pierson FB, Robichaud PR, Spaeth KE. 2001. Spatial and temporal effects of wildfire on the hydrology of a steep rangeland watershed. Hydrological processes, 15: 2905-2916.

Prima SD, Bagarello V, Angulo-Jaramillo R, Bautista I, Crerda A, Campo Ad, Gonzalez-Sanchis M, Iovino M, Lassabatere L, Maetzke F. 2017. Impacts of thinning of a Mediterranean oak forest on soil properties influencing water infiltration. Journal of Hydrology and Hydromechanics 65: 276-286. DOI: 10.1515/johh-2017-0016.

Robichaud PR, Lewis S, Ashmun LE. 2008. New procedure for sampling infiltration to assess post-fire soil water repellency. Res. Note. RMRS-RN-33. Fort Collins, CO: US Department of Agriculture, Forest Service, Rocky Mountain Research Station. 14 p., 33.

Rye C, Smettem K. 2017. The effect of water repellent soil surface layers on preferential flow and bare soil evaporation. Geoderma, 289: 142-149.

Schoennagel T, Balch JK, Brenkert-Smith H, Dennison PE, Harvey BJ, Krawchuk MA, Mietkiewicz N, Morgan P, Moritz MA, Rasker R. 2017. Adapt to more wildfire in

western North American forests as climate changes. Proceedings of the National Academy of Sciences, 114: 4582-4590.

Siegert F, Ruecker G, Hinrichs A, Hoffmann A. 2001. Increased damage from fires in logged forests during droughts caused by El Nino. Nature, 414: 437-440.

Simkovic I, Dlapa P, Doerr SH, Mataix-Solera J, Sasinkova V. 2008. Thermal destruction of soil water repellency and associated changes to soil organic matter as observed by FTIR spectroscopy. Catena, 74: 205-211.

Stewart RD, Abou Najm MR. 2018. A comprehensive model for single ring infiltration. 1: Influence of initial water content and soil hydraulic properties. Soil Science Society of America Journal 82(3): 548-557.

Stoof CR, Wesseling JG, Ritsema CJ. 2010. Effects of fire and ash on soil water retention. Geoderma, 159: 276-285.

Tillman R, Scotter D, Wallis M, Clothier B. 1989. Water repellency and its measurement by using intrinsic sorptivity. Soil Research, 27: 637-644.

Tillman RW, Scotter D, Wallis MG, Clothier B. 1989. Water-repellency and its Measurement by using Intrinsic Sorptivity. Aust J Soil Res, 27: 637-644.

Tobin M, McGhee G, Kroodsma D, Hazzard E. 2016. Wildfires in the United States--Data Visualization EcoWest. org.

Westerling AL, Hidalgo HG, Cayan DR, Swetnam TW. 2006. Warming and earlier spring increase western US forest wildfire activity. science, 313: 940-943.

Woods SW, Balfour VN. 2008. The effect of ash on runoff and erosion after a severe forest wildfire, Montana, USA. International Journal of Wildland Fire, 17: 535-548.

Woods SW, Balfour VN. 2010. The effects of soil texture and ash thickness on the post-fire hydrological response from ash-covered soils. Journal of Hydrology, 393: 274-286.

Woods SW, Birkas A, Ahl R. 2007. Spatial variability of soil hydrophobicity after wildfires in Montana and Colorado. Geomorphology, 86: 465-479.

Yi L, Xin R, Robert H, Malone R, Ying Z. 2017. Characteristics of Water Infiltration in Layered Water-repellent Soils. Pedosphere.

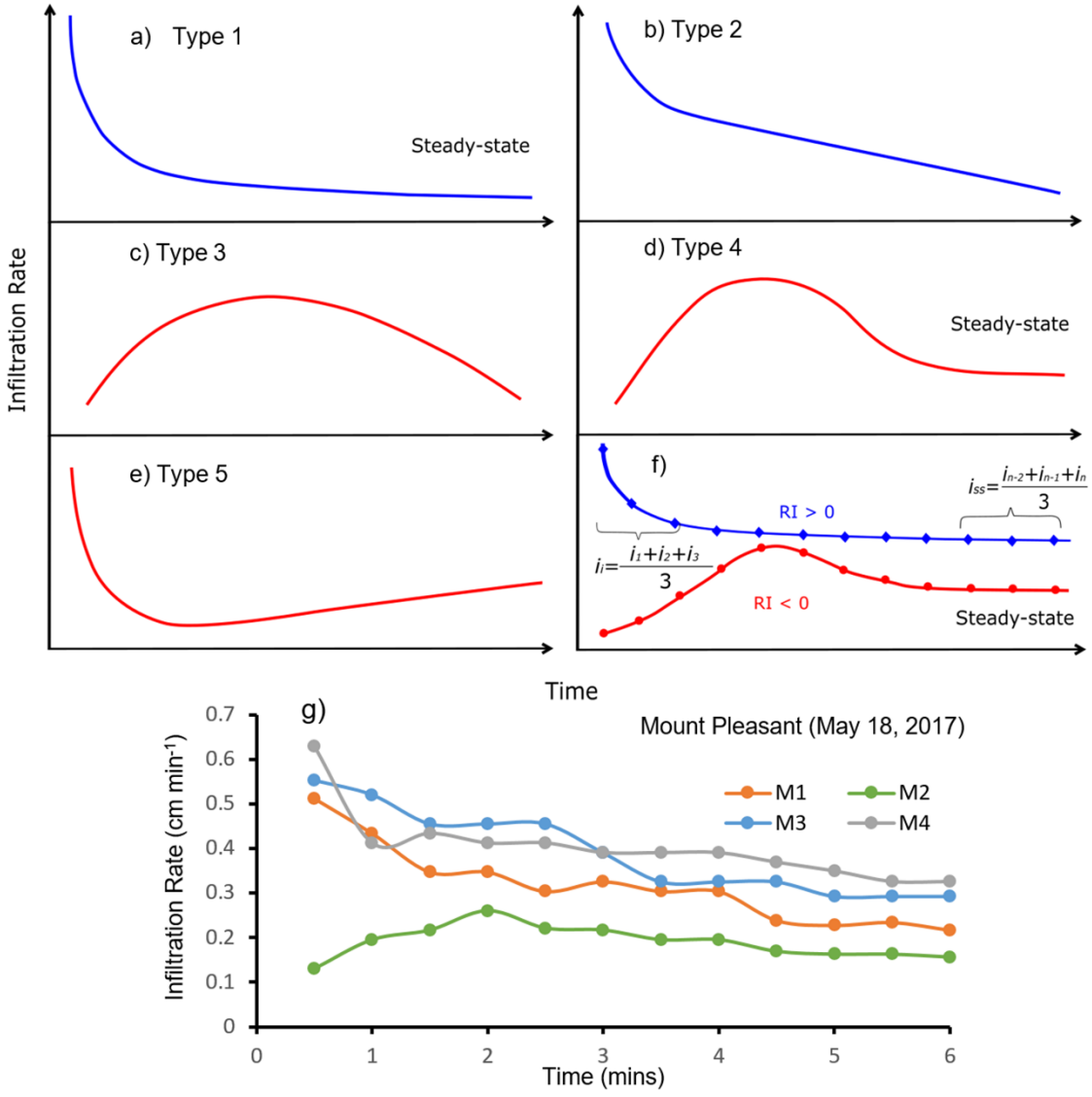

Figure 1: Conceptual infiltration curves for hydrophilic and water-repellent soils, based on previous research by Imeson *et al.* (1992) and Pierson *et al.* (2001): a) Type 1: *exponential decrease*; b) Type 2: *linear decrease*; c) Type 3: *initial increase to decrease*; d) Type 4: *initial increase to steady state*; and e) Type 5: *exponential decrease to linear increase*. Panel f) presents the calculation for relative infiltration (*RI*) based on initial (i_i) and steady-state (i_{ss}) infiltration rates, while Panel g) shows example hydrographs that were collected in the Mount Pleasant location on May 18, 2017. Note that the blue lines in panels a-f represent infiltration curves associated with hydrophilic soil conditions, whereas the red lines indicate water-repellent soil conditions.

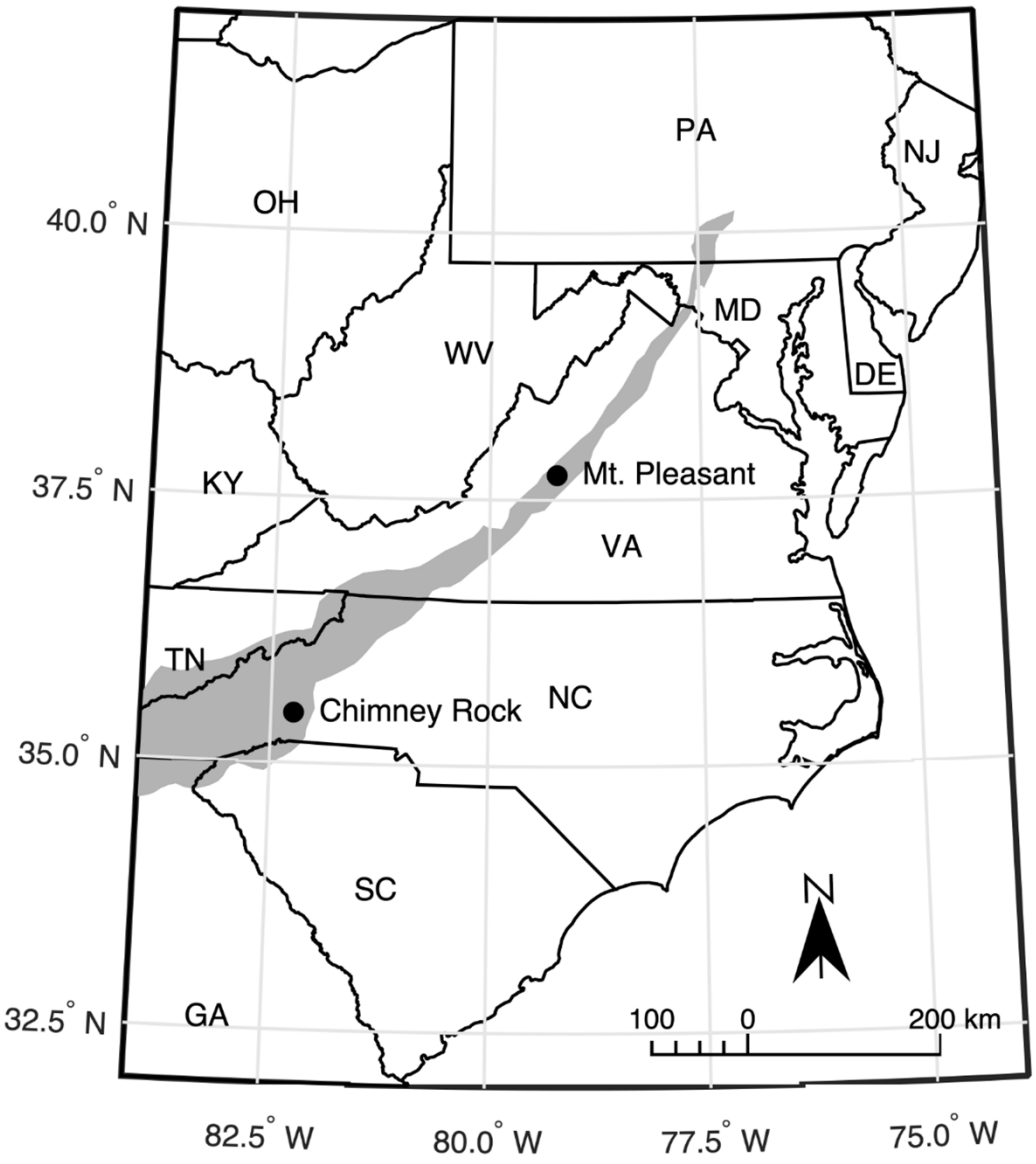

Figure 2: The Blue Ridge physiographic province of the Appalachian Mountains, with the two sampling locations (Mount Pleasant and Chimney Rock) indicated.

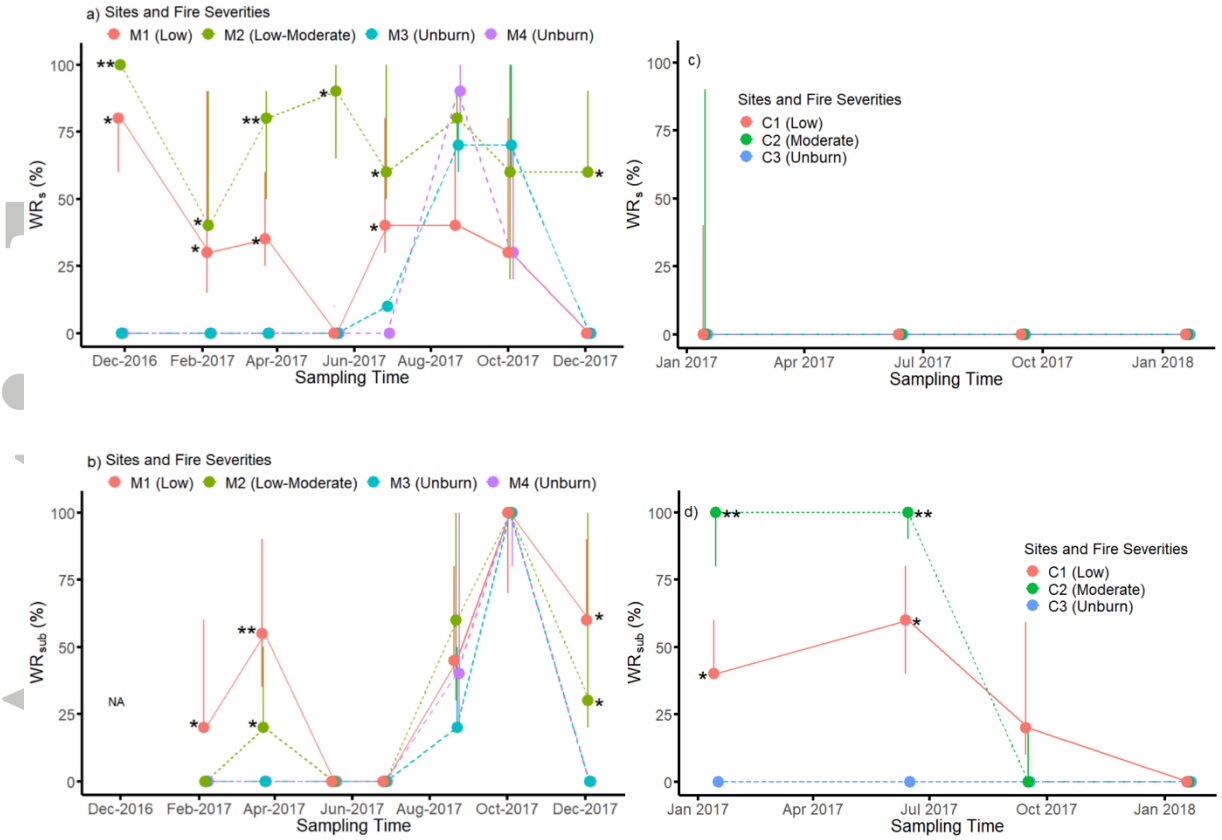

Figure 3: The variations of water repellency in surface (a and c) and subsurface layer (b and d) in each sampling time after wildfires in Mount Pleasant (a and b) and Chimney Rock (c and b). "NA" refers the measurements of WR in subsurface layer in Nov. 2016 in Mount Pleasant were not recorded. Points refer to the median, and Bars indicate 95% confidence intervals. Significant differences between positions (MU, $p < 0.05$) were analyzed. **'s and *'s refer to the significant differences between sites for a particular sampling time (K-W with MU, $p < 0.05$). K-W = Kruskal-Wallis test; MU = Mann–Whitney U test.

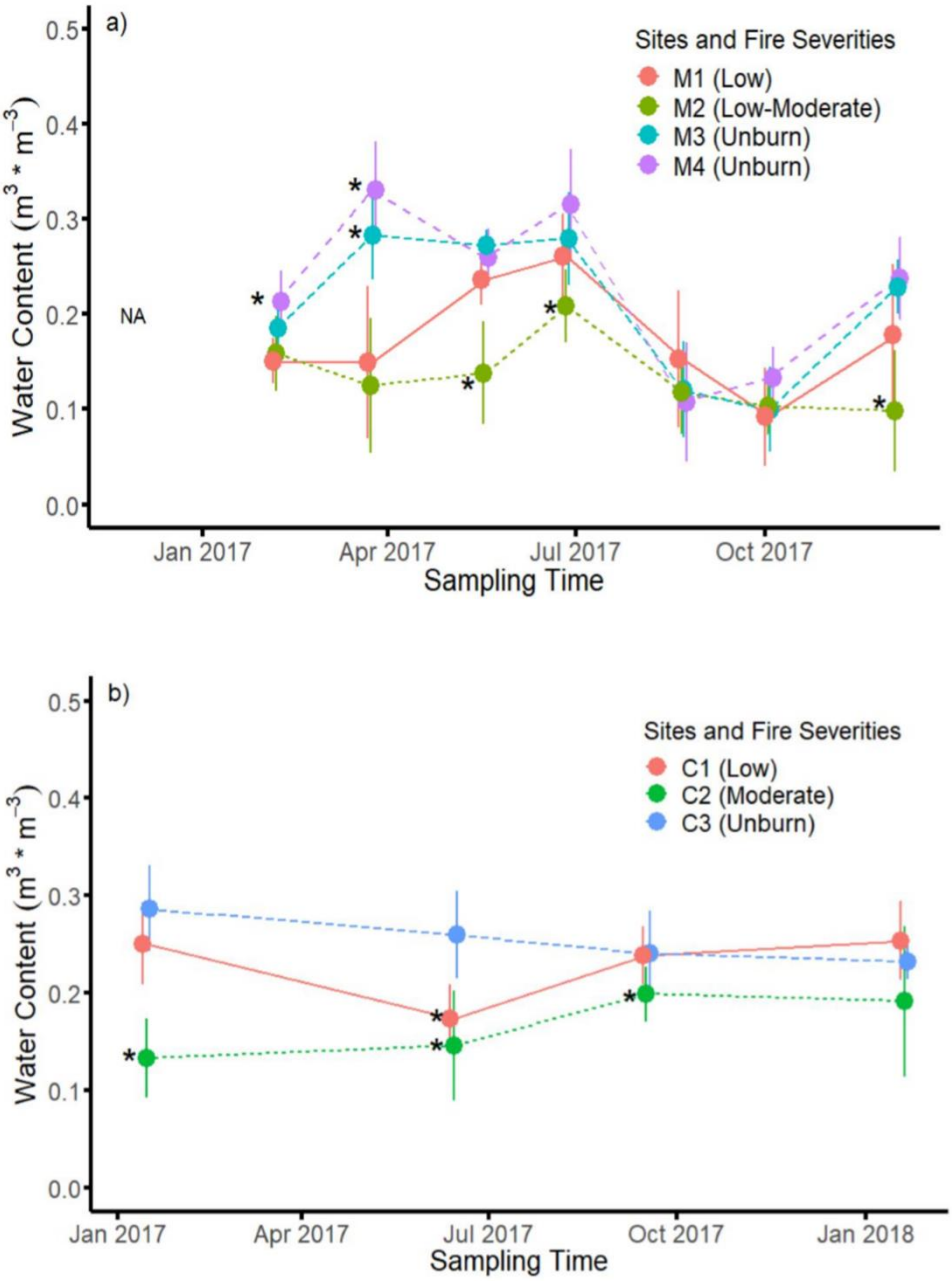

Figure 4: The variations of soil water content in each sampling time after wildfires in Mount Pleasant (a) and Chimney Rock (b). "NA" indicates times when measurements were not recorded. Bars show standard deviations, while * indicates significant differences from other sites within the same sampling time (ANOVA with Tukey's HSD, $p < 0.05$). ANOVA = analysis of variance; HSD = honestly significant difference.

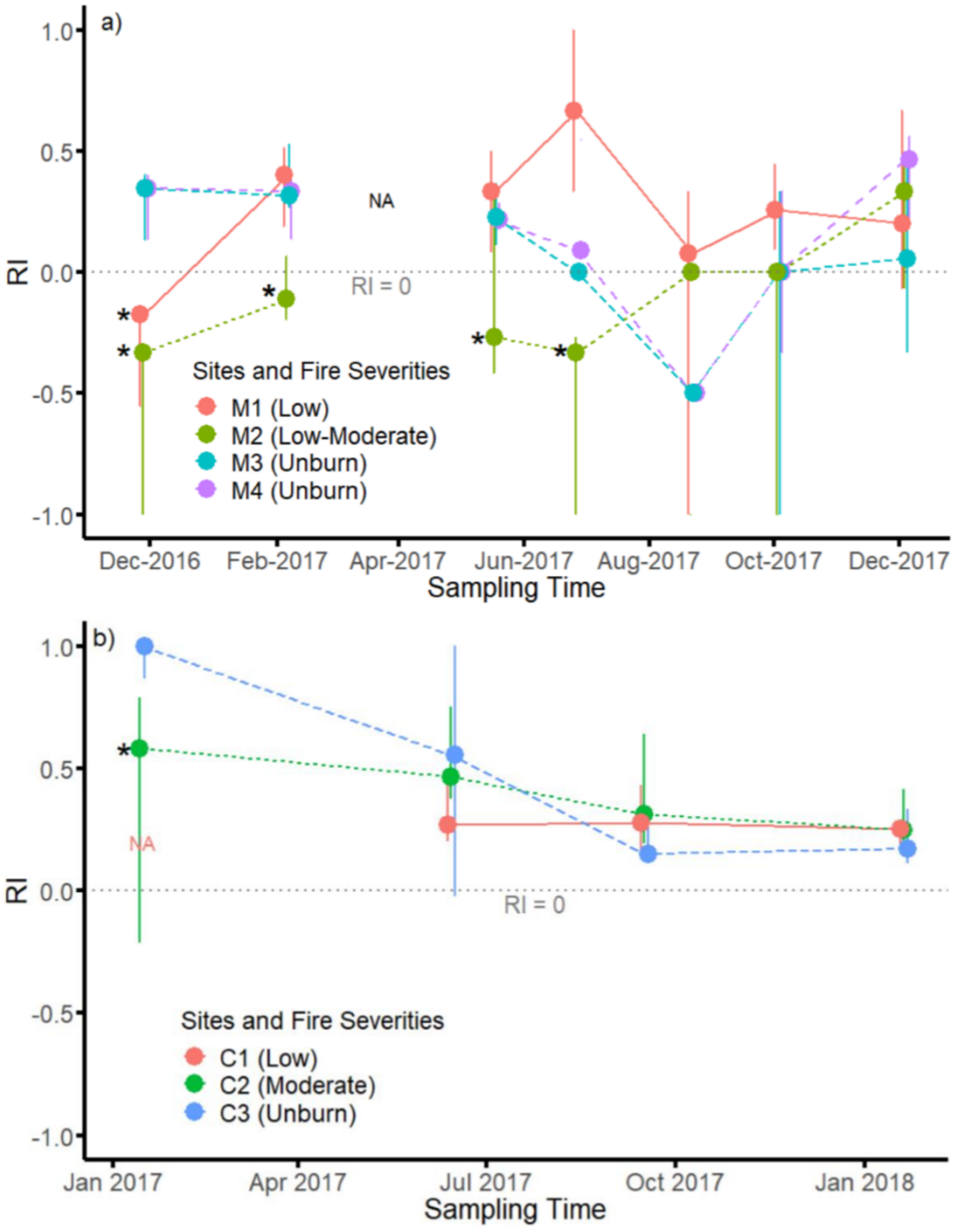

Figure 5: Relative infiltration rates (*RI*) for each sampling time after wildfires in (a) Mount Pleasant and (b) Chimney Rock. "NA" indicates times and sites where measurements were not collected. Points refer to the median and bars indicate 95% confidence intervals, while * indicates significant difference from other sites within the same sampling time (K-W with MU, $p < 0.05$). K-W = non-parametric Kruskal-Wallis test; MU = Mann-Whitney U test.

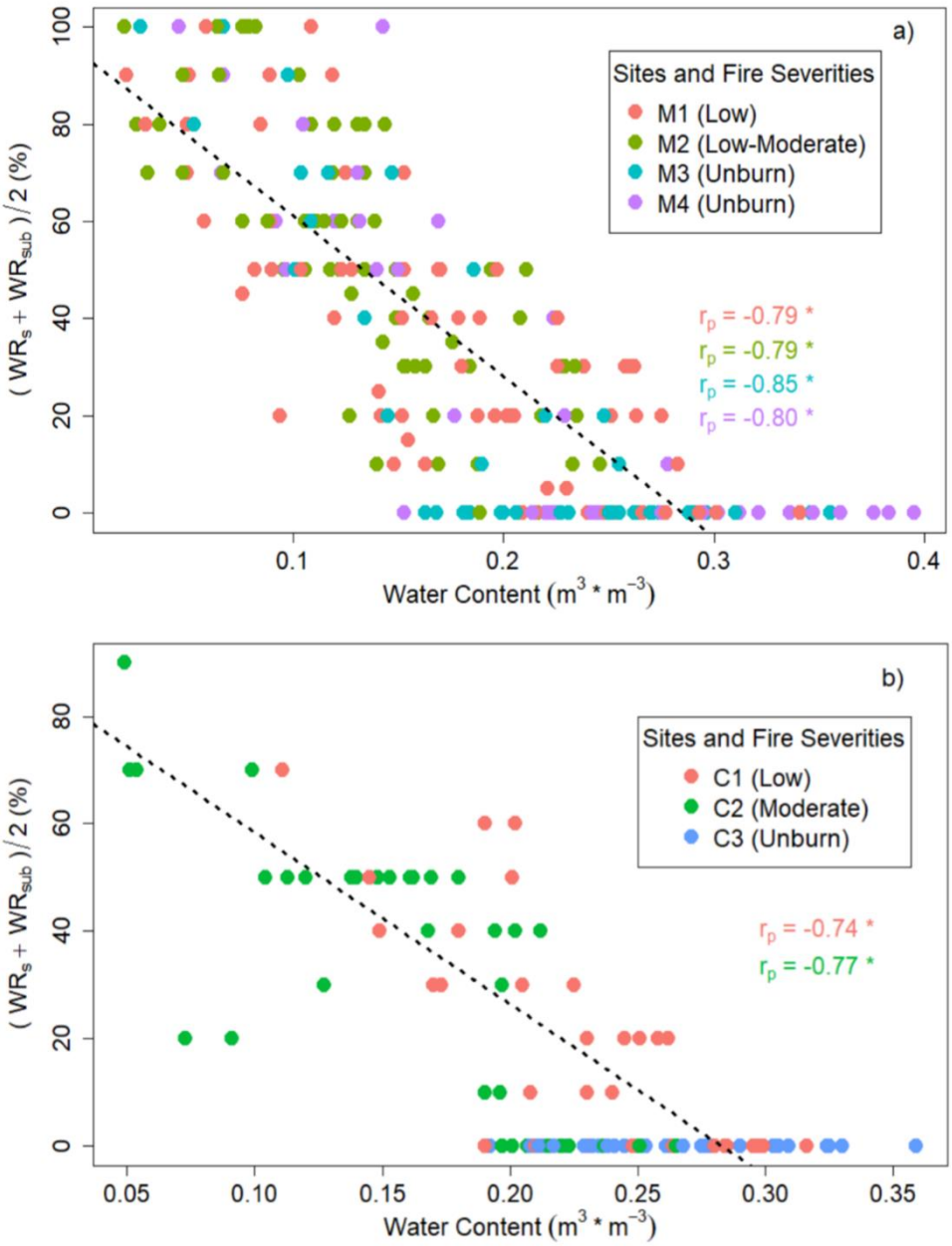

Figure 6: Relationship between soil water repellency (average of surface and subsurface, i.e., (WR_s + WR_{sub})/2) and water content in (a) Mount Pleasant and (b) Chimney Rock. rp refers to the Pearson's correlation coefficient for each site, while * indicates a significant correlation between soil water and water content ($p < 0.05$). Dashed line shows the significant overall linear regression using Analysis of Covariance (ANCOVA); individual linear regression models were not significantly different between sites ($p_{slope} = 0.22$ and $p_{intercept} = 0.42$ in Mount Pleasant; $p_{slope} = 0.17$ and $p_{intercept} = 0.07$ in Chimney Rock).

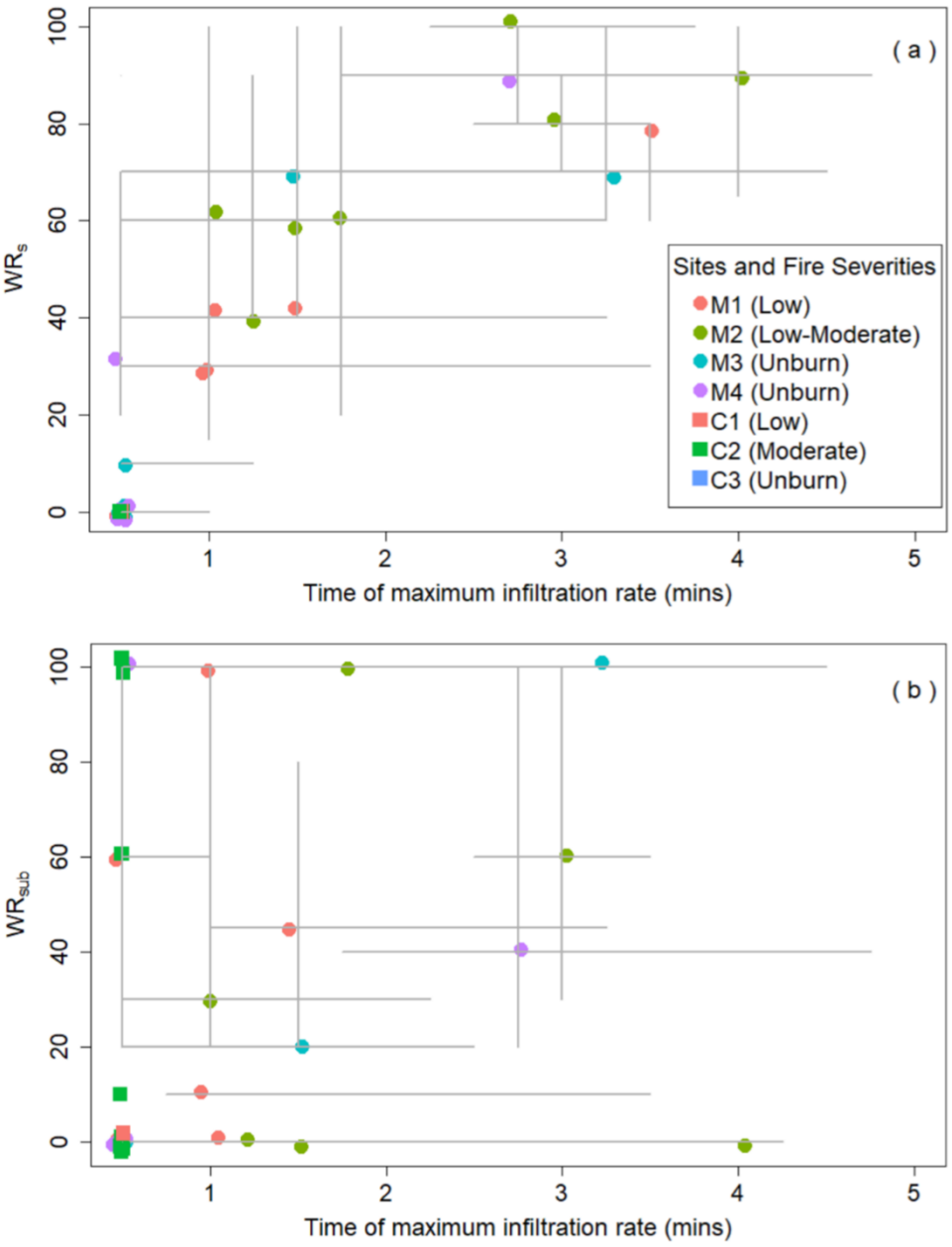

Figure 7: The relationship between the time of maximum infiltration rate (t_{mir}) and water repellency in the (a) surface and (b) subsurface layers. Data come from both sampling locations: Mount Pleasant (M) and Chimney Rock (C). Dots/squares refer to the median, and bars indicate 95% confidence intervals.

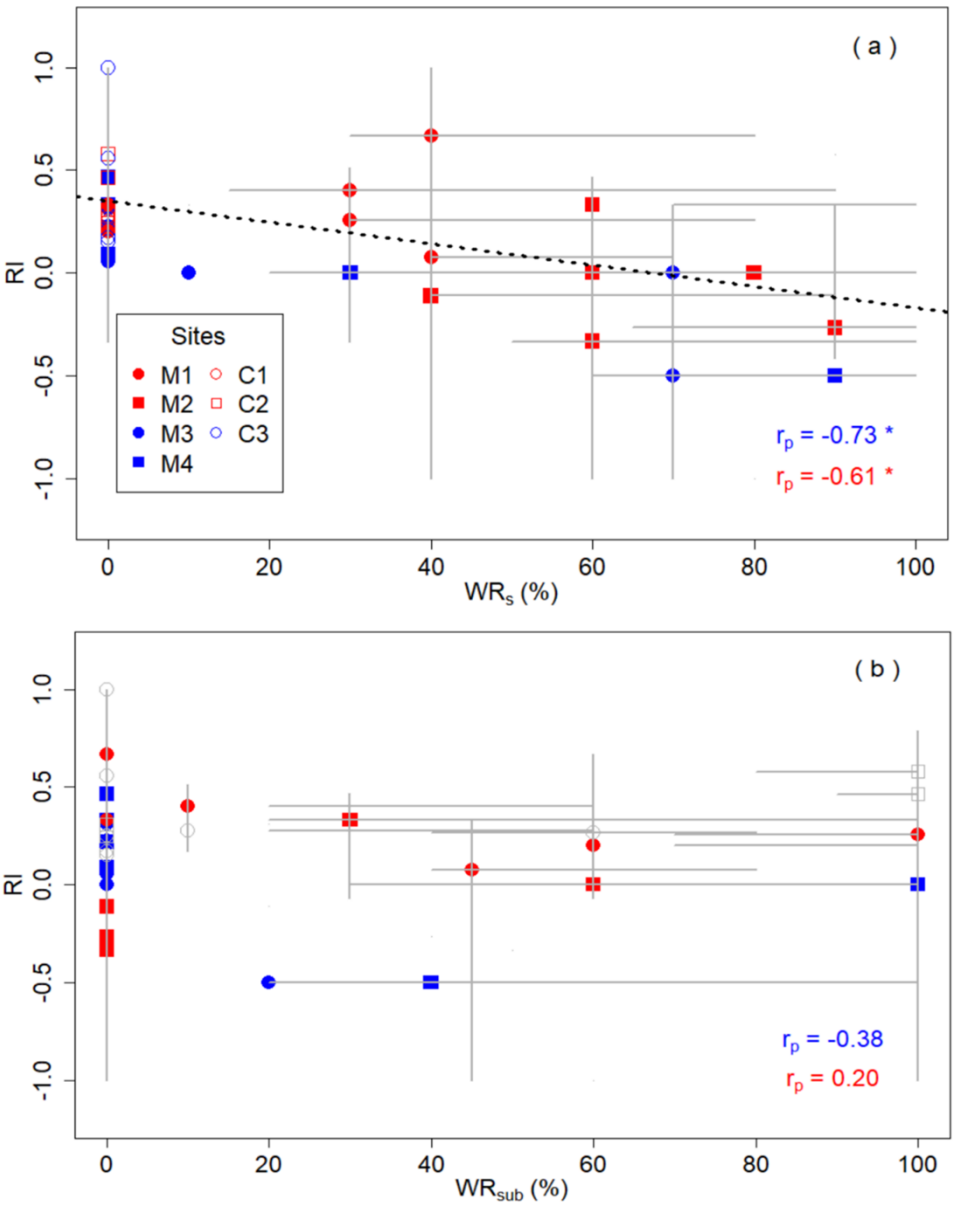

Figure 8: Relationship between relative infiltration rates (*RI*) and water repellency in (a) surface (WR_s) and (b) subsurface layers (WR_{sub}) in Mount Pleasant (M) and Chimney Rock (C). Dots/squares refer to the median, and bars indicate 95% confidence intervals. rp refers to the coefficient of determination using Pearson's correlation coefficient in burned and unburned sites, while * indicates a significant correlation between *RI* and either WR_s or WR_{sub} ($p < 0.05$). Dashed line shows significant overall linear regression using Analysis of Covariance (ANCOVA); individual linear regression models were not significantly different between burned and unburned sites ($p_{slope} = 0.20$ and $p_{intercept} = 0.14$).

Table 1: Summary of soil properties, forest plants species, and wildfire characteristics at the two study locations.

Location	Sites #	Fire Severity	FRPs (MW)	Soil pH	Organic matter content (g*100g^{-1})	soil texture	Bulk density (g*cm^{-1})	Ash thickness (cm)	Plant Species
Mount Pleasant (MP)	M1	Low	16.2	5.5	13.9	Loam	1.30	0.6 ± 0.5	*Quercus rubra, Quercus montana, Kalmia latifolia, Robinia pseudoacacia, Menziesia pilosa, Fraxinus Americana, Juniperus virginiana L., Carya ovata, Betula alleghaniensis, Salix nigra Marsh, Acer rubrum L., Polytrichium* moss, *Potentilla Canadensis, Pteridium aquilinum, Monotropa uniflora, Castanea dentate, Aureolaria laevigata, Cornus alternifolia*
	M2	Low - Moderate		5.3	16.1		1.27	2.1 ±1.1	
	M3	Unburned		5.0	8.3		1.45	-	
	M4	Unburned		4.6	13.3		0.92	-	
Chimney Rock (CR)	C1	Low	90.6	5.1	7.1	Sandy Loam	1.41	1.1 ± 0.8	*Quercus rubra, Quercus montana, Acer rubrum, Quercus coccinea, Liriodendron tulipifera, Carya alba, Carya glabra, Pteridium aquilinum, Sassafras albidum, Kalmia latifolia,*
	C2	Moderate		5.3	4.4		1.47	4.6 ±3.2	
	C3	Unburned		4.8	11.6		1.27	-	